Dynamical theory of low-energy ionization of inert-gas atoms at surfaces

Y. Muda* and D. M. Newns†
Imperial College, London SW7, United Kingdom
(Received 17 July 1987)

A quasi-*ab-initio* calculation of the ionization probability of a low-energy He atom at the surface of a linear chain of n atoms (modeling Si) has been made using the technique of numerical solution of the equations of motion for $\mathcal{N}_{ij}(t) \equiv \langle \Psi_S(t) | c_i^\dagger c_j | \Psi_S(t) \rangle$. The low-energy-ionization effect below 1 keV has been explained on the basis of impact scattering, in which the projectile valence orbital overlaps the target core orbitals. Two conditions are established for seeing the effect: (1) The hopping integral $V_{ak}(z)$ between the orbitals centered on the He atom and the target atom must go through zero at distances $z \simeq R_C$ (the distance of closest approach). (2) The diabatic level centered on the projectile must shift up to near ε_F there. Fortunately, the first condition will be rather generally encountered, because of the oscillations in the target valence orbitals at small radius. On the other hand, feature (2) is more specific to the projectile-target material combination and leads to some target material dependencies. At energies higher than 2 keV, the ionization probabilities with and without the level shift Δ become identical, and only condition (1) is necessary. Thus, in this energy region the surface ionization effect will be more generally expected for such systems as, e.g., the He→Cu surface, which has a noncrossing energy-level diagram or $\Delta = 0$, in good agreement with experiment. For energies greater than 50 or 100 keV, neither condition is necessary, and P_{ion} oscillates as a function of E_0, representing the quasiresonant ionization process. It is also found that the ionization probability P_{ion} in surface scattering ($n \geq 30$) is nearly 1 order of magnitude greater than that in a binary collision ($n = 1$), at an energy of 1 keV. The effect of the energy-band occupation has also been shown to be of essential importance.

I. INTRODUCTION

The charge-exchange probability of reflected atoms at solid surfaces is very important in surface analysis techniques such as ion-beam scattering spectroscopy (ISS), neutral-beam scattering spectroscopy (NSS), or secondary-ion mass spectroscopy (SIMS). Several theoretical descriptions of low-energy ion neutralization processes at surfaces have been developed.[1–7] Most of them are based on the time-dependent Anderson model. A review is given by Newns *et al.*[8] Very little is known, however, about the way in which ionization of noble-gas atoms at surfaces occur at energies below 1 keV (NSS).

As regards experiments on (re)ionization of He atoms at surfaces, some interesting results have been reported.[9–12] Verhey *et al.*[9] found an ionization probability of 2% at 3 keV increasing to 30% at 10 keV for He atom→Cu(100) surface collision. In ISS, Souda *et al.*[10] found that a He atom which was neutralized on the incoming trajectory can be reionized with a large probability even at energies below a few hundreds of eV. Low-energy ionization of neutral He atoms at energies below 2 keV has also been found for the target elements C, Na, Mg, Si, K, Ca, Ti, Mn, Sr, Y, Zr, Mo, Sn, Sb, Te, and Ta, but not for F, Cl, Co, Ni, Cu, Zn, Ge, Ag, Cd, In, I, and Pb.[11] These experiments stimulated the present study.

Here we briefly review the experimental results of Souda *et al.*[10,11] The energy spectra of He^+ ions scattered by a TaC(0001) surface consisted of two peaks, A and B. Peak A was thought to be due to elastic binary collision between He and Ta atoms. Peak B lies about 20 eV below peak A. The energy loss $\delta E \simeq 20$ eV is independent of incident energy E_0 and azimuthal angle ψ. It is nearly equal to the difference between the He $1s$ level ($\simeq -24.6$ eV) and the Fermi level ε_F ($\simeq -4.5$ eV) of the substrate. From these facts, they interpreted peak B as caused by those He^+ ions which were Auger neutralized into the $1s$ state on the incoming trajectory and then reionized at the surface, an electron in the He $1s$ level being promoted to one of unfilled valence levels of the substrate. In order to confirm the above interpretation, they measured the ion fraction of neutral He atoms scattered from the surface (NSS). The measured energy spectra of reflected He^+ ions were identical to peak B in ISS. The intensity of peak B relative to that of peak A, I_B/I_A, considered as a function of E_0, had an onset threshold around $E_0 \simeq 500$ eV. Moreover, the occurrence of peak B, or the ion peak in NSS, had the target-material dependence mentioned above, for $E_0 < 2$ keV.[11]

More recently, however, Thomas *et al.*[12] obtained scattered He-ion spectra in NSS for all the 16 elements Al, Si, Cr, Fe, Co, Ni, Cu, Mo, Pd, Ag, Cd, In, Sn, Ta, W, and Au from 1-, 1.5-, and 2-keV incident neutral He beams. Results for Si, Mo, Sn, and Ta targets agree with the result by Souda and Aono,[11] but disagree for Co, Ni, Cu, Ag, Cd, and In targets. Note that the result by

Verhey *et al.*[12] also shows that ionization occurs for He→Cu(100) at 3 keV.

Thus, some disagreement remains in the experimental results on target-material dependence, but the low-energy ionization effect at surfaces itself is interesting, because the threshold energy is so low. From conventional electron transition theory between two levels which are separated by $\delta E \simeq 20$ eV, the cross section for charge transfer will be maximum at a relative velocity v_0 such that the Massey factor $a \mid \delta E \mid /\hbar v_0 \simeq 1$, where a is the distance over which both atoms interact. If we use approximate values of $v_0 = 0.1$ a.u. (or, $E_0 = \frac{1}{2} m_{\mathrm{He}} v_0^2 = 1002$ eV), $\delta E = 1$ a.u., and $a = 2$ a.u., the Massey factor amounts to 20. For the Massey factor to be unity, v_0 must be 2 a.u., or $E_0 \simeq 400$ keV.

The Massey criterion may be satisfied, however, even in such cases, (1) if there is a "promotion" of the He 1*s* level during the collision so that it crosses the target valence-band states (effective reduction of δE), and (2) if there is a rapid change of $V_{ak}(z)$ near impact, which causes an effective increase of v_0. These two effects will be considered in this paper.

As regards electron promotion, two levels of the same symmetry avoid crossing in an adiabatic transition as is well known. Hence, Lichten *et al.*[13,14] introduced the concept of the "diabatic" level. The diabatic correlation diagram of Barat and Lichten[14] (BL) is drawn by conserving the number of radial nodes, $n - l$, between the separated and united atom states. Using this concept, many experimental results in the field of atomic collisions were explained.[14]

Although there is no unique definition of the "diabatic molecular-orbital," it is also apparent that the adiabatic molecular-orbital basis set would be unsuitable for treating the collision problem. Among many proposals for calculating the diabatic orbitals,[15–17] a simple and reasonable one is the (distorted) frozen-orbital (FO) method of Gauyacq.[15,16] In it, the linear combination of atomic orbitals (LCAO) coefficients of each molecular orbital (MO) are frozen at a certain point R_G, beyond which the diabatic MO's are required. The FO method enables the neglect of d/dR coupling and is able to reproduce the BL diabatic correlation diagram. The simplest diabatic FO basis set is the frozen atomic orbital (FAO).[18] It corresponds to $R_G = \infty$, and has proved to be useful for treating excitation process at high energies.[18] Here we also work with the diabatic orbital in the simplest FAO method. The diabatic orbital we consider emerges from the He 1*s* level at $z = \infty$ and correlates with the S 3*d* level at $z = 0$. More details will be given in Sec. II.

Recently, based on the electron promotion model, Tsukada *et al.*[19,20] have made configuration-interaction (CI) calculations of the molecular orbitals of a large number of diatomic molecules He-*X* as functions of internuclear distance, where *X* stands for an element in the Periodic Table, and discussed the target-material dependence obtained by Souda and Aono.[11] As the MO calculation gives only stationary states that avoid crossing, they determined the diabatic level crossing by inspection, and obtained two groups of atoms (*X*), one having diabatic level crossings as in Fig. 2(a), and the other no crossing as in Fig. 2(b). The results coincided with the experimental target-material dependencies of Souda and Aono.[11] For example, no diabatic level crossing was found for the HeCu molecule. However, in the experiments by Verhey *et al.*[9] and Thomas *et al.*,[12] significant ionization probabilities were observed for the He→Cu surface case. This discrepancy between the experimental and theoretical results indicates that the diabatic level crossing is not sufficient to explain the whole phenomenon of low-energy ionization at surfaces, although it will be one of the important conditions. To obtain a complete view of the effect over a wider energy range, a more direct dynamical theory needs to be developed.

In this paper, we consider the low-energy ionization effect for a He atom at a Si surface by solving a quantum-mechanical equation of motion of the electron system without any adiabatic approximation. The motion of a He atom along its trajectory is explicitly treated, and the energy bands of the substrate, electron hopping interaction between colliding atoms, and so on, are taken into account as realistically as possible. This is the first attempt at semi-*ab-initio* calculation of the charge-exchange process at surfaces.

II. MODEL

We consider the charge-transfer process between a He atom and the solid surface in the trajectory approximation. As in the theories[1–8] of ion neutralization near the surface, the electron system is described by a spinless time-dependent Anderson model Hamiltonian,

$$\mathcal{H}(t) = \varepsilon_a(t) n_a(t) + \sum_k \varepsilon_k n_k + \sum_k [V_{ak}(t) c_a^\dagger c_k + \mathrm{H.c.}] , \tag{2.1}$$

where the first term represents a He atom with the frozen atomic orbital $\phi_a = \phi_{1s}$ whose energy $\varepsilon_a(t)$ is a function of $z(t)$, as shown in Fig. 1. $z(t)$ is the internuclear distance between the He atom and the target atom. The second term in Eq. (2.1) represents the substrate, and the third the interaction between them. $n_a = c_a^\dagger c_a$ and $n_k = c_k^\dagger c_k$, where $c_a^\dagger$, c_a, $c_k^\dagger$, and c_k are the creation and annihilation operators for an electron in the states ϕ_a and ϕ_k, respectively. ε_k and ϕ_k are the energy eigenvalues and eigenstates of the substrate Hamiltonian $\mathcal{H}^0$, respectively, which will be given in Eqs. (2.4) and (2.5).

In Fig. 1, the energy-level diagram is shown schematically, where the He 1*s* level is to be thought of as a diabatic state, which correlates with the sulfur 3*d* level in the united atom limit, obeying the constant $(n - l)$ rule. At large distances z from the surface, $\varepsilon_a(z)$ is assumed to lie -20 eV below ε_F, and to rise as z decreases up to $\varepsilon_{s\,3d} \simeq 3.7$ eV above ε_F.[21] The total level shift Δ is about 23.7 eV.[21] This corresponds to the correlation diagram of Fig. 2(a), in which there is the $3d\sigma - 3s\sigma$ MO crossing. In Fig. 2(b), the diabatic correlation diagram for He + Cu→Ga is also shown, where the He 1*s* level correlates with the Ga 3*d* level which lies at almost the same level with the He 1*s* level. Here there is no crossing, and $\Delta \simeq 0$ in this case.

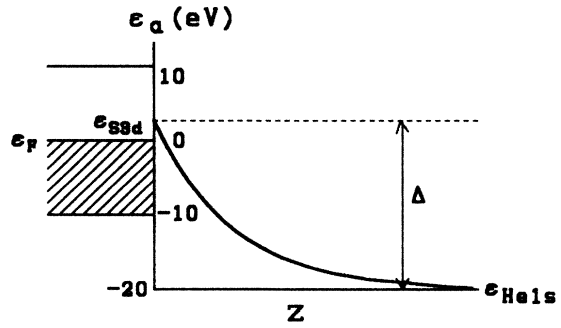

FIG. 1. Schematic energy-level diagram

We assume an exponential variation of ε_a as a function of z as follows:

$$\varepsilon_a(t)=\varepsilon_0+\Delta\exp[-z(t)/z_a]\ , \tag{2.2}$$

where z_a is a characteristic distance associated with the level shift. We assumed that $z_a=2$ a.u. from the MO level diagram of a HeSi molecule, in which case the diabatic He $1s$ level crosses ε_F at $z\simeq 0.34$ a.u.

The substrate is represented by a tight-binding linear chain of atoms, assuming that there is an orthonormal Wannier orbital $\phi_i(r)$ on each atomic site $1\le i\le n$. We choose the energy of ϕ_i as the origin of energy. Only the nearest-neighbor (NN) hopping integral β is taken into account. Then the substrate Hamiltonian is represented as follows:

$$\mathcal{H}^0_{ij}=\begin{cases}\beta & \text{for } i-j=1\\ 0 & \text{for } i-j\neq 1\ ,\end{cases} \tag{2.3}$$

where i and j indicate atomic site in the substrate. The exact eigenvalues ε_k and eigenfunctions ϕ_k of this Hamiltonian are[22]

$$\varepsilon_k=2\beta\cos[k\pi/(n+1)],\quad k=1-n \tag{2.4}$$

$$\phi_k(\mathbf{r})=[2/(n+1)]^{1/2}\sum_i \sin[ik\pi/(n+1)]\phi_i(\mathbf{r})\ . \tag{2.5}$$

These ε_k and ϕ_k are used in Eq. (2.1).

$V_{ak}(t)$ in Eq. (2.1) represents the hopping integral between ϕ_{1s} and ϕ_k. Using Eq. (2.5) gives

$$V_{ak}(t)=\int\phi_{1s}(\mathbf{r}-z(t)\mathbf{i})\mathcal{H}(t)\phi_k(\mathbf{r})dv$$
$$=[2/(n+1)]^{1/2}\sin[k\pi/(n+1)]V(z(t))\ , \tag{2.6}$$

where

$$V(z)=\int\phi_{1s}(\mathbf{r}-z\mathbf{i})\mathcal{H}(t)\phi_1(\mathbf{r})dv\ , \tag{2.7}$$

$\mathbf{i}$ is the unit vector normal to the surface, and ϕ_1 the Wannier orbital centered on the target atom. Interactions between the He atom and the other substrate atoms are neglected.

The hopping integral $V(z)$ in Eq. (2.7) has been calculated using the self-consistent-field (SCF) atomic wave functions for He and Si atoms given by Herman-Skillmann[23] as shown in Fig. 3. Further, we approximated them by the following analytical expressions.

Model I: An exponential form

$$V(z)=V_{as}\exp[-z(t)/z_a]\ . \tag{2.8}$$

Fitting Eq. (2.8) to the true matrix elements $\langle$He $1s\,|\,\mathcal{H}\,|$ Si $3s\rangle$ and $\langle$He $1s\,|\,\mathcal{H}\,|$ Si $3p_z\rangle$ in the region $z>1.5$ a.u. yields $V_{as}=2.5$ a.u. and $z_a=1.6$ a.u., which is shown in Fig. 3. The behavior of the true hopping integrals is fairly well represented in the region $z>1.5$ a.u., but very poorly in the core region $z<1.5$.

Model II: Gaussian form

$$V(z)=V_{as}\exp\{-[z(t)/z_a]^2\}\ . \tag{2.9}$$

Fairly good fitting is obtained by $V_{as}=1.2$ a.u. and $z_a=3.2$ a.u. in the region $z>1.5$ a.u. as in the case of model I [Eq. (2.8)], but the behavior in the core region $z<1.5$ a.u. is still poorly represented.

Model III: A nodal form

$$V(z)=V_{as}\gamma\exp(1-\gamma)\ , \tag{2.10}$$

where

$$\gamma=[z(t)/z_a]^q\ . \tag{2.11}$$

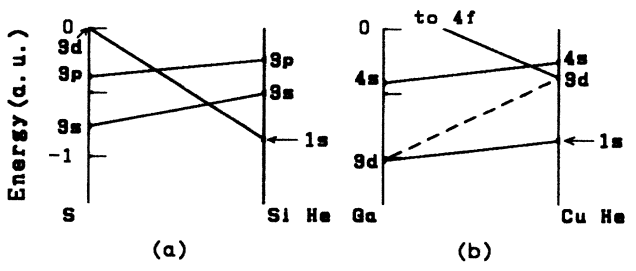

FIG. 2. Diabatic correlation diagram for (a) He + Si, and (b) Cu + He. The $3d\,\sigma$–$3s\,\sigma$ and $3d\,\sigma$–$3p\,\sigma$ crossings are shown in (a).

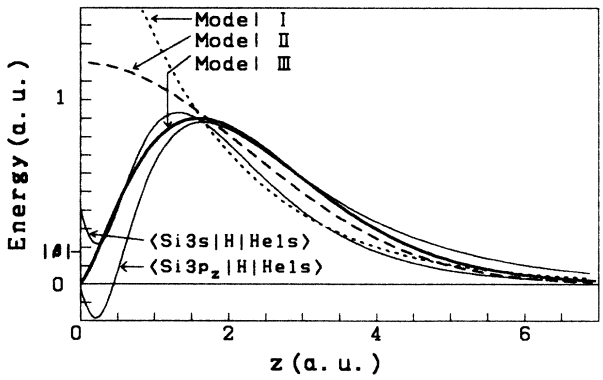

FIG. 3. Hopping integrals $\langle$He $1s\,|\,\mathcal{H}\,|$ Si $3s\rangle$ and $\langle$He $1s\,|\,\mathcal{H}\,|$ Si $3p_z\rangle$ have been calculated using the SCF atomic orbitals and potentials given by Herman and Skillmann (Ref. 23), and three analytic approximations to them, as functions of internuclear distance z.

The $V(z)$ in Eq. (2.10) has a node at $z=0$ as $\langle$ He $1s \mid \mathcal{H} \mid$ Si $3p_z \rangle$ does exactly and $\langle He\ 1s \mid \mathcal{H} \mid$ Si $3s \rangle$ does approximately. The decrease in the latter matrix elements in the region $z<1.5$ a.u. is due to the quasiorthogonality of the He $1s$ orbital and the Si $3s$ or $3p_z$ orbitals in the united atom limit. Therefore, this behavior in $V(z)$ of model III can be expected for other substrate materials as well. $V(z)$ in Eq. (2.10) with $V_{as}=0.9$ a.u., $z_a=1.6$ a.u., and $q=1.3$ is closely identical to those of the exact matrix elements $\langle$ He $1s \mid \mathcal{H} \mid$ Si $3s \rangle$ and $\langle$ He $1s \mid \mathcal{H} \mid$ Si $3p_z \rangle$ in the entire region of z.

The reason why these three models of interaction were examined is as follows: Model I was examined first, but did not give an appreciable ionization effect at low energies around $E_0=500$ eV (see Fig. 6, curve I). So, model II was examined next, but the results were also discouraging (see Fig. 6, curve II). Finally, model III was examined, and found to give a clear ionization effect at low energies as seen in Fig. 6, curve III.

The trajectory of the He atom is approximated by the following hyperbolic curve:

$$z(t)=[R_C^2+(v_0 t)^2]^{1/2} , \tag{2.12}$$

where z is the internuclear distance between the He atom and the target atom, v_0 the relative initial velocity, and R_C the distance of closest approach. The trajectory is calculated using a Molière potential, for the scattering angle 130° ($\phi_C=50°$) as a function of the incident energy E_0 (see Fig. 4). It is seen that R_C in the region of $E_0 \leq 1$ keV is approximated well by the following expression:

$$R_C=12.92E_0^{-0.5319} , \tag{2.13}$$

where R_C is in atomic units ($\simeq 0.53$ Å) and E_0 in eV.

In solving the equation of motion in the next section, we represented the trajectory of a He atom by Eqs. (2.12) and (2.13), neglecting the polar angle dependence of the trajectory. Equation (2.12) is better than the discontinuous linear trajectory approximation $z(t)=R_C+v_0 \mid t \mid$, which is poor in the vicinity of $z \simeq R_C$.

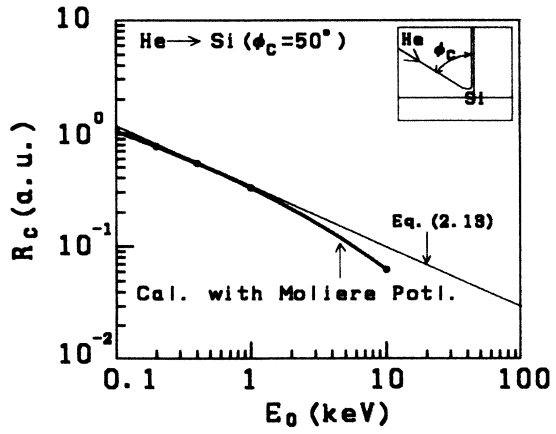

FIG. 4. The distance of closest approach R_C as a function of the incident energy E_0. The solid curve is calculated using a Molière potential for He→Si ($\phi_C=50°$). The straight line is an analytic approximation to it [Eq. (2.13)].

III. METHOD OF CALCULATION

The system is described by the Schrödinger equation:

$$i\hbar\frac{\partial \Psi_S(t)}{\partial t}=\mathcal{H}(t)\Psi_S(t) , \tag{3.1}$$

where $\mathcal{H}(t)$ is given by Eq. (2.1). The initial state is assumed to be represented by a determinantal wave function given by the equation

$$\mid \Psi_S(t=-\infty)\rangle = \mid \phi_{1s\uparrow}(1)\phi_{1s\downarrow}(2)\phi_{k_0\uparrow}(3)\phi_{k_0\downarrow}(4)\cdots\phi_{k_F\downarrow}(n_F)\rangle , \tag{3.2}$$

which represents the system where the He $1s$ orbital is occupied by a pair of electrons and the orbitals ϕ_k in the substrate are also occupied by a pair of electrons up to the Fermi level ε_F. Then the probability of the He atom being ionized in the final state will be given by the equation

$$P_{\text{ion}}=1-\langle \Psi_S(t=\infty) \mid c_a^\dagger c_a \mid \Psi_S(t=\infty)\rangle , \tag{3.3}$$

where spin degeneracy is neglected.

As our aim is to calculate P_{ion}, only the final value of $\langle n_a(t)\rangle$ for $t\to\infty$ is needed. Hence, instead of solving Eq. (3.1), which is impossible, the equation-of-motion method, originally proposed by Muda and Hanawa[3] in a calculation of the neutralization probability of a low-energy He^+ ion scattered by a surface, is used here: Defining the occupation number matrix $\mathcal{N}_{ij}(t)$ by the equation

$$\mathcal{N}_{ij}(t)\equiv\langle \Psi_S(t) \mid c_i^\dagger c_j \mid \Psi_S(t)\rangle , \tag{3.4}$$

its time derivative is given by the equation

$$i\hbar\frac{d\mathcal{N}_{ij}(t)}{dt}=\langle \Psi_S(t) \mid [c_i^\dagger c_j,\mathcal{H}(t)]_- \mid \Psi_S(t)\rangle . \tag{3.5}$$

Substituting $\mathcal{H}(t)$ of Eq. (2.1) into Eq. (3.5) gives

$$i\hbar\frac{d\mathcal{N}_{ij}(t)}{dt}=\sum_n h_{jn}(t)\mathcal{N}_{in}(t)+h_{ni}(t)\mathcal{N}_{nj}(t) , \tag{3.6}$$

where the $h_{ij}(t)$'s stand for matrix elements of the Hamiltonian $\mathcal{H}(t)$ in Eq. (2.1). Equation (3.6) represents a set of coupled first-order differential equations for $\mathcal{N}_{ij}(t)$, which can be solved numerically by methods such as the Runge-Kutta-Gill routine. The initial value of $\mathcal{N}_{ij}(t=-\infty)$ corresponding to the initial state in Eq. (3.2) is given by the following equations:

$$\begin{aligned} &N_{aa}(t=-\infty)=1 , \\ &N_{kk}(t=-\infty)=\begin{cases}1 & \text{for } \varepsilon_k \leq \varepsilon_F \\ 0 & \text{for } \varepsilon_k > \varepsilon_F\end{cases} , \\ &N_{kk'}(t=-\infty)=0 \quad \text{for } k\neq k' , \\ &N_{ak}(t=-\infty)=0 . \end{aligned} \tag{3.7}$$

IV. RESULTS

In Fig. 5, the time variation of $\mathcal{N}_{aa}(t)$, the occupation number of the diabatic orbital ϕ_a centered on the incident He atom, is shown for incident energies $E_0=0.5$, 1, 10, and 100 keV, for the case of $\beta=-5$ eV (bandwidth of 20 eV), $\varepsilon_F=0$ (half-filled band), $\varepsilon_a(t)=-20+23.67\exp[-z(t)/2]$ eV, $V(t)=-0.9\gamma\exp(1-\gamma)$ a.u., where $\gamma=[z(t)/1.6]^{1.3}$ and $z(t)$ in a.u., for example. The integration of Eq. (3.6) was done using a Runge-Kutta-Gill routine, starting at $z=8$ a.u. with $dt=0.013\,33/v_0$ until the variation of $\mathcal{N}_{aa}(t)$ becomes smaller than 10^{-6}, where v_0 is the incident velocity of the He atom. We note that, at $z=8$ a.u., $V(z)$ in Eq. (2.10) is less than 0.006 a.u., so that the effect of the sudden switch on of V_{ak} is negligible. Other effects such as the finite chain length have also been checked carefully. Some of these effects are described in Sec. IV D.

At $t\simeq-\infty$, $\mathcal{N}_{aa}(t)$ is nearly equal to unity, representing the fact that the He atom was neutral initially. When it approaches the surface, $\mathcal{N}_{aa}(t)$ begins to decrease due to the mixing of the He 1s level with the band states. In the case of $E_0=500$ eV in Fig. 5(a), $\mathcal{N}_{aa}(t)$ is very close to, say, the adiabatic curve (dashed one), which is the solution of the steady-state Schrödinger equation $\mathcal{H}\Psi=\varepsilon\Psi$ with the He atom fixed at the point corresponding to time t. Therefore, only a small ionization probability is found in this case, although even that is much greater than the ones obtained with model I or II, as can be seen in Fig. 7. In the cases of high incident velocities in Figs. 5(b), 5(c), and 5(d), on the contrary, $\mathcal{N}_{aa}(t)$ deviates from the adiabatic curve significantly. The deviation grows with time t, resulting in a large ionization probability.

The present ionization effect will be self-evidently expected in the case of high velocities $v_0>1$ a.u. (or, $E_0>100$ keV for He), but not in the case of low velocities $v_0<0.1$ a.u. ($E_0<1$ keV for He), where the nuclear motion is nearly 1 order of magnitude slower than the electronic orbital motion. So we looked for the conditions for the low-energy ionization effect to occur at surfaces, by making extensive calculations with various parameters.

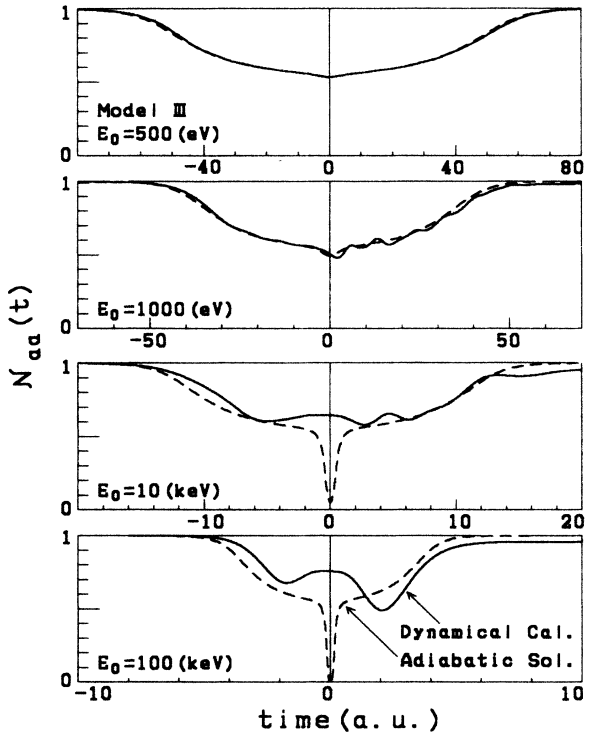

FIG. 5. Time variation of the electron occupation number $\mathcal{N}_{aa}(t)$ of the orbital ϕ_a centered on the He projectile. E_0 is the incident energy. The solid curves are the results of numerical integration of Eq. (3.6), and the dashed curves the solutions of the steady-state Schrödinger equation $\mathcal{H}\Psi=\varepsilon\Psi$ with the He atom fixed at the distance $z(t)$.

A. Comparison between models of the interaction $V(z)$

In Fig. 6, P_{ion} is shown as a function of incident energy $E_0=\frac{1}{2}m_{\text{He}}v_0^2$ for the three models of the He-Si hopping integral $V(z)$ mentioned in Sec. III, for the case of $\Delta=0.87$ a.u. ($\simeq 23.7$ eV), $\beta=-5$ eV, and $\varepsilon_F=0$. It is clearly seen that models I and II are quite unfavorable for ionization in the region $E_0<10$ keV, whereas model III has a steep onset in P_{ion} around $E_0\simeq 500$ eV and shows an appreciable ionization probability of the order of 1% at $E_0=1$ keV. The order of magnitude agrees with experiment, although the experimental determination of the absolute value of the ionization probability is said to be difficult at present.

In Figs. 7 and 8, the behavior of $\mathcal{N}_{aa}(t)$ is compared for the three models at $E_0=1$ and 4 keV, respectively. In model III, "ringing" of $\mathcal{N}_{aa}(t)$ around the adiabatic curve is seen, which becomes clearer at higher E_0 as shown in Fig. 8. This ringing of the system will be closely connect-

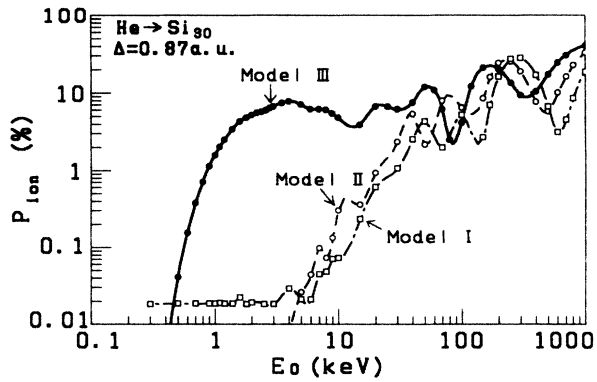

FIG. 6. Calculated ionization probability P_{ion} as a function of the incident energy E_0 for $\Delta=0.87$ a.u., $\beta=-5$ eV, and $\varepsilon_F=0$ (half-filled band). The three curves are the results with the hopping integrals $V(z)$ of models I, II, and III shown in Fig. 3 and given by Eqs. (2.8), (2.9), and (2.10), respectively. The number (n) of atoms in the linear chain of the substrate is 30.

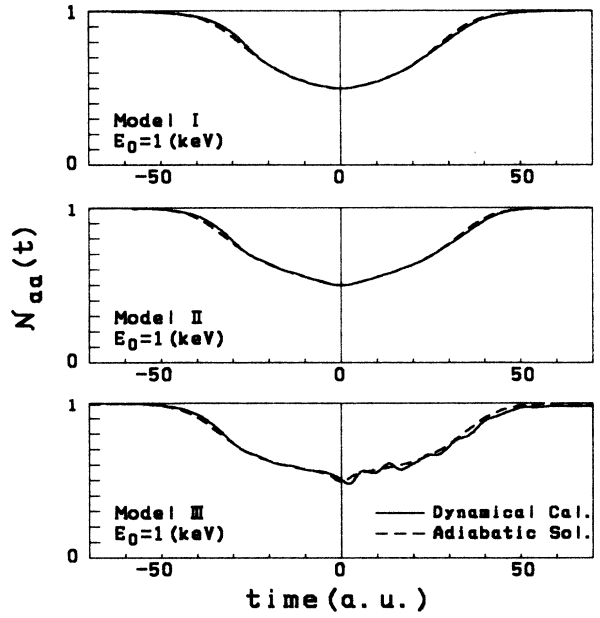

FIG. 7. Comparison of the behavior of $\mathcal{N}_{aa}(t)$ for the various models I, II, and III, at $E_0=1$ keV (see figure caption of Fig. 5).

ed to the high ionization probability of model III. We first note, however, that the ringing is not of artificial origin such as finite chain length or sudden switching on of V_{ak}.

Here, we consider the reason why model III is so favorable compared with models I and II. Note that the $V(z)$'s of models I and II are very large in the region $z<1.5$ a.u. (Fig. 3). On the other hand, the $V(z)$ of model III decreases towards zero in this region, and becomes comparable with β near $z\simeq 0.2$ a.u.

If $|V(z)| \gg |\beta|$ as in models I and II, the electron hopping between the target Si atom and the He atom is much stronger than the hopping between the target Si atom and the nearest-neighbor Si atom in the substrate, so that the system at that internuclear distance z is just like a HeSi molecule which is weakly coupled to the remainder of the substrate. This is endorsed by Fig. 9: The local densities of states (LDOS) at the He and the target Si-atom sites consist of the bonding and antibonding split-off states far below and above the valence band. At the second Si-atom site, however, the LDOS is like that of the free surface. In other words, the system is nearly equal to a binary collision system, because of the relationship $|V(z)| \gg |\beta|$ near $z\simeq R_C$.

If $|V(z)| \simeq |\beta|$ as in model III, on the other hand, an electron can hop into the remainder of the substrate, that is, the presence of the remainder of the substrate plays a role. Thus the two cases are in sharp contrast: The former (models I and II) is nearly an atomic collision (He→Si), while the latter (model III) is a true surface scattering. By the way, in Sec. IV D (Fig. 12), it will be shown that the ionization probability for the atomic collision is nearly 1 order of magnitude smaller than that in the surface collision. Thus one reason why models I and II are unfavorable is thought to be that the effect of the substrate vanishes due to the fact that $|V(z)| \gg |\beta|$ near $z\simeq R_c$ in models I and II. Why should the atomic collision be less effective in ionization of the He atom than the surface collision? At present we only note the fact that, in an atomic collision, an electron is confined within the pair of atoms; on the other hand, in a surface collision, it can hop into the remainder of the substrate.

Another reason why model III is favorable but models I and II are not is as follows: There is a rapid change of $V_{ak}(z)$ near impact as seen in Fig. 3. In other words, a sudden kick occurs when $V(z)$ changes from much less than the bandwidth to much greater than the bandwidth

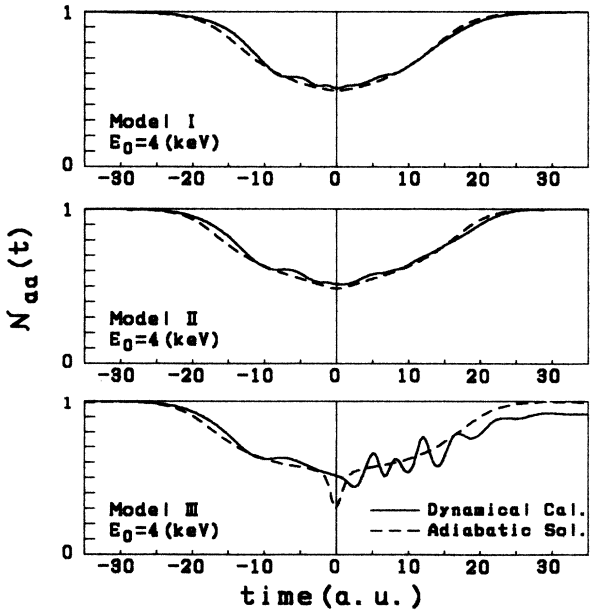

FIG. 8. Comparison of the behavior of $\mathcal{N}_{aa}(t)$ for the various models I, II, and III, at $E_0=4$ keV (see figure caption of Fig. 5).

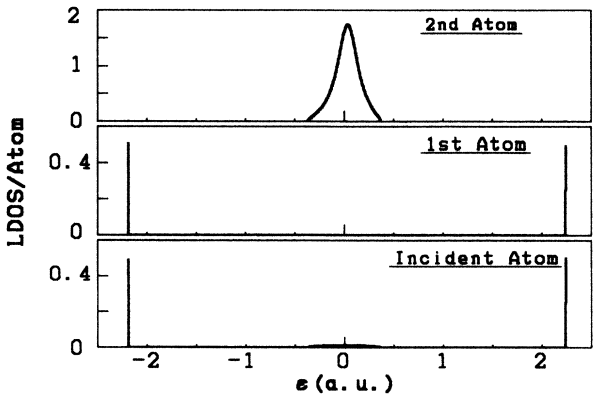

FIG. 9. The local density of states at (a) the second Si, (b) the first Si, and (c) the incident He atom sites, obtained as the solution of $\mathcal{H}\Psi=\varepsilon\Psi$ at $z=0.2$ a.u. where the $V(z)$ of model I has been employed.

in a short time. Specifically, $V(z)$ of model III changes from -7.5 eV ($t=0$) to -14.1 eV ($t=5$ a.u.) in a time $\tau=5$ a.u. (1 a.u. $=2.419\times10^{-21}$ sec), at $E_0=1$ keV. At 4 keV, it changes from -3.1 eV ($t=0$), to -21.2 eV ($t=5$ a.u.). On the other hand, $V(z)$ of model II only changes from -32.7 eV ($t=0$) to -29.6 eV ($t=5$ a.u.), even at $E_0=4$ keV. This rapid change of V_{ak}, which is encountered only in model III, causes an increase of the velocity v_0, effectively satisfying the Massey criterion.

In any case, the large P_{ion} at low energies in the case of model III can be ascribed to the decrease in $V(z)$ around $z\simeq R_C$ to a value comparable with or less than β, the NN hopping integral in the substrate. Thus the first condition for seeing the low-energy-ionization effect at surfaces is as follows.

Condition (1). The hopping integral $V(z)$ between the orbitals centered on the projectile and the target atom must not be much greater than the NN hopping integral β in the substrate at distances $z\simeq R_C$.

Fortunately, this condition will be met more or less generally as mentioned in Sec. III. Therefore, the low-energy-ionization effect can be expected more or less generally for many target materials, although there can be some target-material dependencies arising from the level shift effect, which is more specific to the combination of the projectile and the target materials, as will be mentioned in Sec. IV C. This prediction agrees well with the recent experimental results of Thomas *et al.*,[12] who found ionization for all target elements they tried. In the experiment by Souda and Aono,[11] the target-material dependencies are prominently demonstrated below $E_0=2$ keV, but that does not rule out the possibility that ionization would occur at E_0 greater than 2 keV for those elements for which they did not find an appreciable effect.[24] In fact, Verhey *et al.*[9] also found ionization probabilities even for the He→Cu surface case. This point will be discussed again in Sec. IV C.

B. I_B/I_A

In order to make a more quantitative comparison between the theory mentioned above and experiment, we calculated I_B/I_A from the results in Fig. 6, where I_A and I_B are intensities of the elastic and energy loss peaks, respectively. The experimental results for I_B/I_A by Souda and Aono[10] are reproduced in Fig. 10. Theoretical values of I_A and I_B were calculated as follows: I_A is thought to represent the intensity of ions which have survived neutralization in the course of scattering, so that it is given by the equation

$$I_A=P_S^{\text{I}}P_S^{\text{II}}I_0\ , \tag{4.1}$$

where I_0 represents the incident ion intensity, and P_S^{I} and P_S^{II} are the survival probabilities of a He^+ ion on the incoming and outgoing trajectories, respectively. I_B represents the intensity of ions which are once neutralized in the incoming path, then ionized by the collision, and finally, surviving neutralization on the outgoing trajectory, reach the detector. It is represented by the equation

$$I_B=(1-P_S^{\text{I}})P_{\text{I}}P_S^{\text{II}}I_0\ , \tag{4.2}$$

where P_I represents the ionization probability on collision, for which we use the P_{ion} in Fig. 6. Using Eqs. (4.1) and (4.2), the ratio I_B/I_A is given by the equation

$$I_B/I_A=[(1-P_S^{\text{I}})/P_S^{\text{I}}]P_I\simeq P_I/P_S^{\text{I}}\ . \tag{4.3}$$

We further assume that P_S^{I} is given by the equation

$$\begin{aligned}P_S^{\text{I}}&=\exp(-v_C/v_0)\\&=\exp[-(E_C/E_0)^{1/2}]\ ,\end{aligned} \tag{4.4}$$

where v_C and E_C are the characteristic velocity and energy, respectively. The exponential form of Eq. (4.4) has been assumed to be valid both for Auger and resonance neutralization processes. E_C is determined by fitting the theoretical value for I_B/I_A at $E_0=1$ keV with the experimental value. Then the P_{ion} versus E_0 in Fig. 6 can be transformed into the form of I_B/I_A as shown in Fig. 10.

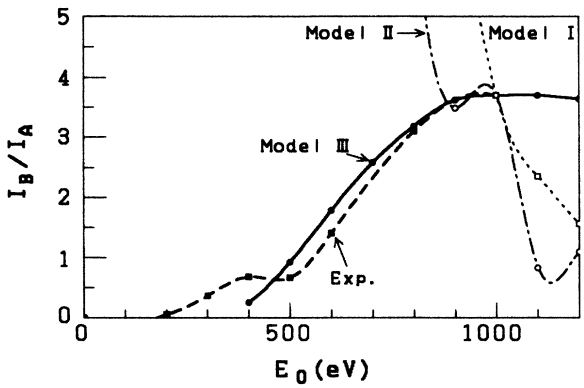

FIG. 10. I_B/I_A as a function of the incident energy E_0. The dotted, dot-dashed, and solid curves are calculated using the values of P_{ion} presented in Fig. 6, based on the assumption mentioned in the text, for models I, II, and III, respectively. The dashed curve is the experimental result by Souda and Aono (Ref. 11) for He→Ti on the TiC(1000) surface.

Note that only model III gives good agreement with experiment as before. Comparison between the results of model I or II and experiment is very poor: I_B/I_A of models I and II tend to increase with decreasing E_0. This shows that the I_B/I_A versus E_0 plot is a severe test of the model.

C. Effect of level shift Δ

In Fig. 11, P_{ion} versus E_0 with $\Delta=0.87$ a.u. (solid curve) and 0 eV (dashed curve) are plotted; the hopping integral of model III is employed. In the low-energy region of $E_0<2$ keV, P_{ion} for $\Delta=0.87$ a.u. is nearly 1 order of magnitude larger than that for $\Delta=0$. An ionization probability greater than 0.1% is found at $E_0\simeq500$ eV. This suggests the second condition for seeing the low-energy-ionization effect at surfaces.

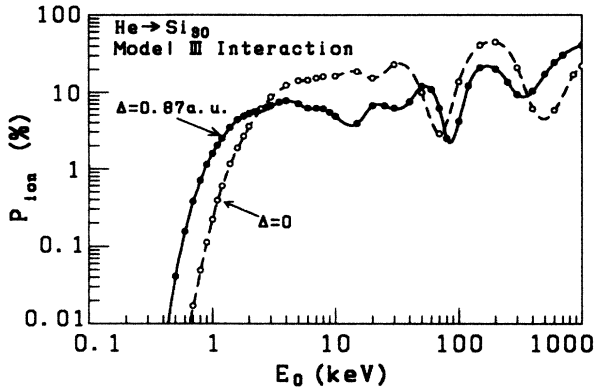

FIG. 11. Calculated ionization probabilities P_{ion} as functions of the incident energy E_0 with the level shift $\Delta=0.87$ a.u. and $\Delta=0$. [$\beta=-5$ eV, $\varepsilon_F=0$, and the hopping integral is that of model III, or Eq. (2.10).]

Condition (2). The diabatic level centered on the projective shifts up to the Fermi level ε_F near $z\simeq R_C$.

This condition is equivalent to the requirement that the system has a diabatic level crossing as in Fig. 2(a). Note that $\Delta=0.87$ and 0 correspond to Figs. 2(a) and 2(b), respectively.

On the other hand, in the intermediate-energy region from 2.5 to 50 keV, where $v_0\simeq 0.15$–0.7 a.u., P_{ion} with $\Delta=0$ is rather greater than that with $\Delta=0.87$ a.u. (Fig. 11). In this energy region, the level shift Δ is unnecessary, although condition (1), mentioned in Sec. IV A, is still necessary, as can be seen from Fig. 6. The curves of models I and II in Fig. 6 lie much lower than that of model III in the energy region of $E_0<30$ keV.

The fact that P_{ion} can amount to a significant value even with $\Delta=0$ is very important. It implies that the low-energy-ionization effect at surfaces will occur quite generally if the incident energy E_0 exceeds ~ 2 keV, even for a target-projectile material combination that has a noncrossing diabatic correlation diagram like Fig. 2(b). Thus we have reached a very important conclusion that ionization below ~ 2 keV will occur if both conditions (1) and (2) are satisfied [the second condition requires the system to have a crossing correlation diagram like Fig. 2(a)], but above ~ 2 keV, the ionization will occur if only the first condition is satisfied. Therefore, we can expect the effect even in such cases as the He→Cu surface which has the noncrossing correlation diagram of Fig. 2(b). In earlier work, there has been the assumption[11,20] that if a system has a noncrossing energy-level diagram, then low-energy ionization will not occur. But, this statement may give us the erroneous impression that the ionization will never occur in such a system. The present calculation has clearly proved that even such a system definitely has a significant ionization probability from one percent to several tens of percent, in the region above $\simeq 2$ keV. This prediction agrees well with the experimental results.[9–12] As mentioned in Sec. IV A, Souda and Aono's experiment[11] clearly indicates the existence of target-material dependencies in the energy region below 2 keV, but this does not mean that such a system will never show the ionization effect above 2 keV. We hope that more experiments will be done for such systems above 2 keV in the future.

In the high-energy region $E_0\geq 100$ keV, where v_0 exceeds 1 a.u. so that the Massey factor $a\Delta E/\hbar v_0<2$ (for $a\simeq 2$ a.u., $\Delta E\simeq 1$ a.u.), both curves for $\Delta=0.87$ a.u. and $\Delta=0$ become identical and oscillate sinusoidally. Even the curves of models I and II ($\Delta=0.87$ a.u.) in Fig. 6 also show high ionization probabilities in this energy region. This means that neither condition is necessary in this energy region. The sinusoidal oscillation in P_{ion} as a function of $1/v_0$ is characteristic of a resonant charge transfer. Thus the oscillation in P_{ion} found in Figs. 6, 11, and 12 for $E_0\geq 100$ keV represents the quasiresonant ionization process. As $v_0\simeq 1$ a.u. and $a\simeq 1$ a.u., the energy uncertainty δE amounts to about 1 a.u. ($\simeq 27.3$ eV). Thus the diabatic level even 20 below ε_F is in quasiresonance with the valence band due to the energy uncertainty. The quasiresonant neutralization mechanism has been discussed by Bloss and Hone.[2]

D. Comparison between surface scattering and atomic scattering

In Fig. 12, P_{ion}'s for $n=1$, 30, and 100 are shown, where $\Delta=0.87$ a.u., and the model-III hopping integral is employed; n is the number of Si atoms in the substrate linear chain. Note that the result for $n=100$ coincides closely with the result for $n=30$. Therefore we regard the results at $n=30$ as representing the semi-infinite linear chain. Hence almost all the results presented in this paper are those at $n=30$.

It is seen in Fig. 12 that P_{ion} at $n\geq 30$ (solid curve) is larger than that of $n=1$ by nearly 1 order of magnitude, in the energy region of $E_0\simeq 10$ keV. As $n=1$ corresponds to an atomic collision, the difference between the results at $n=1$ and $n=30$ represents the difference between an atomic scattering event and a surface scattering

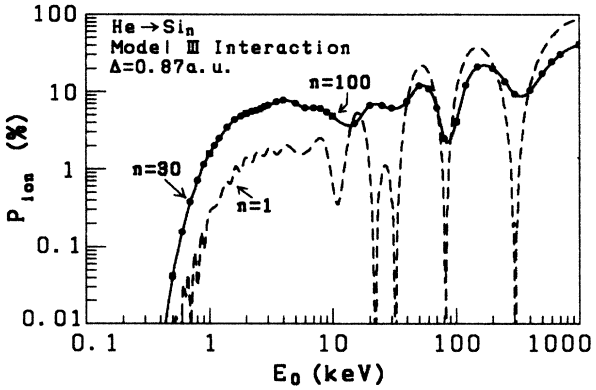

FIG. 12. Calculation ionization probabilities P_{ion} as functions of the incident energy E_0 for $n=1$, 30, and 100, where n is the chain length of the substrate. The results for $n=100$ are shown by solid squares, at six points of E_0. ($\beta=-5$ eV, $\varepsilon_F=0$, and the hopping integral is that of model III.)

event. Figure 12 shows that the ionization probability at low energies will be much larger in surface scattering than in atomic scattering.

In the high-energy region $E_0 > 10$ keV, both curves of $n=1$ and $n=30$ become comparable, although there is a strong oscillation in the $n=1$ curve, arising from the quasiresonant charge transfer between the pair of atoms.

E. Effect of energy-band occupation

Finally, the effect of the energy-band occupation is examined. In Fig. 13, the energy diagrams of the models calculated are shown schematically. Model (a) is the one which has been mainly treated so far. Models (b) and (c) differ from (a) in the value of ε_F, but $\varepsilon_0-\varepsilon_F$ and Δ remain the same as those of model (a). In models (d) and (e), the position of ε_0 relative to the center of the band, and Δ, remain the same as those of model (a), but the band occupation (i.e., ε_F) changes.

In Fig. 14, P_{ion} is shown as a function of ε_F, where $E_0=1$ keV, $\Delta=0.87$ a.u., and the $V(z)$ of model III is employed. Points a–e correspond to the models in Fig. 13, respectively. The valence band of the substrate extends from -10 to 10 eV, thus $\varepsilon_F=-5$, 0, and 10 eV, for example, means a quarter-occupied, half-occupied, and fully occupied band, respectively. It is seen that in the series of *a*, *b*, and *c*, there is a relatively weak dependence on ε_F. In the series of *a*, *d*, and *e*, on the contrary, a strong dependence on ε_F is observed. The comparison shows that an important condition for a high ionization probability at low energy is that the band occupation is as low as possible and the diabatic energy level centered at the incident atom shifts up above ε_F as much as possible.

V. CONCLUSIONS

A quasi-*ab-initio* calculation of the charge-exchange probability has been made which takes into account the motion of the incident He atom scattered by the surface.

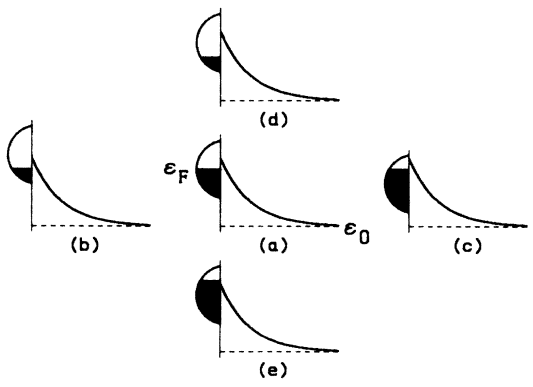

FIG. 13. Schematic energy-level diagrams of the models employed to investigate the effect of the band occupation (see Fig. 14). Model (a) is the one which has been treated in Figs. 6, 11, and 12. The model-III hopping integral, $\Delta=0.87$ a.u., and $n=30$ are employed. Only the relative position of ε_0 and the band occupation vary in these models.

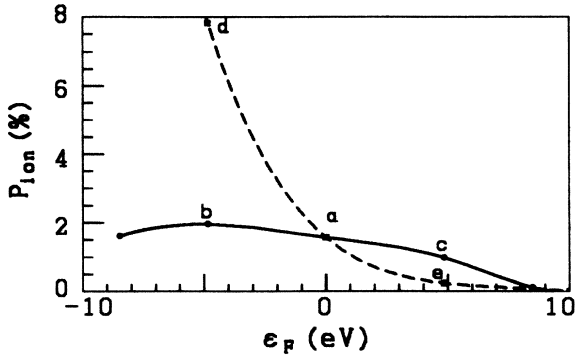

FIG. 14. Ionization probabilities P_{ion} as a function of ε_F at $E_0=1$ keV. Points $a-e$ correspond to the models shown in Fig. 13.

The low-energy-ionization effect, which seems so surprising on the basis of the Massey criterion, has been explained with reasonable assumptions which incorporate ideas from atom-ion scattering theory. We work with a diabatic He 1*s* level whose behavior is determined from the projectile-target correlation diagram. Quasirealistic hopping matrix elements and a He trajectory based on a Molière potential are employed.

The ionization probability P_{ion} has been found to amount to a significant value at low energies even less than 1 keV, if the following conditions are encountered. (1) The hopping integral $V(z)$ between the He 1*s* orbital and the valence orbital centered on the target atom decreases so as to be comparable with the NN hopping integral β in the substrate, at distances $z \simeq R_C$ (the distance of closest approach). (2) The diabatic level centered on the projectile shifts up to near ε_F there. Fortunately, the first condition will be rather generally encountered, because of the quasiorthogonality between the orbitals centered on the incident atom and the target atom in the united atom limit, and also because $V_{ak}(z)$ at $z=0$ is associated with high-quantum-number target states. On the other hand, the feature (2) is more specific to the projectile and target material combination. Thus, although there are some target-material dependencies in the threshold energy, the low-energy-ionization effect at surfaces can be expected more or less generally for many target materials. This prediction combines all of the experimental results presented so far.[9–12]

At energies higher than 2 keV, the ionization effect takes place with and without the level shift Δ: Only condition (1) is necessary. Thus, in this energy region, the surface ionization effect will be more generally seen for almost all target materials, including cases such as the He→Cu surface case which has a noncrossing energy-level diagram as shown in Fig. 2(b) (i.e., $\Delta=0$), in good agreement with experiment.[9,12]

For energies greater than 50 or 100 keV, neither condition is necessary, and P_{ion} amounts to the order of 10%, oscillating as a function of E_0. In this energy region, quasiresonant ionization takes place.

It is also found that the ionization probability P_{ion} in surface scattering ($n \geq 30$) is nearly 1 order of magnitude

greater than that in the binary collision ($n=1$), at $E_0=1$ keV. The effect of the energy band occupation has also been shown to be of essential importance.

The present study is not a full *ab initio* calculation, but the method originally proposed in Ref. 3 can be applied to a much more realistic time-dependent Hamiltonian, so that we hope more realistic calculations of the dynamic properties of surfaces will be made in the future.

ACKNOWLEDGMENTS

One of the authors (Y.M.) thanks Professor Wolfarth and his co-workers at I.C. for their hospitality during the preparation of the present work. Some of the calculations were made on a FACOM 680 computer at the Institute of Molecular Science, Okazaki, Japan.

---

*On leave from Nara University of Education, Takabatake, Nara City 630, Japan.

†Permanent address: IBM Thomas J. Watson Research Center, P.O. Box 218, Yorktown Heights, NY 10598.

[1]A. Blandin, A. Nourtier, and D. Hone, J. Phys. (Paris) **37**, 369 (1976).

[2]W. Bloss and D. Hone, Surf. Sci. **72**, 277 (1978).

[3]Y. Muda and T. Hanawa, Surf. Sci. **97**, 283 (1980).

[4]R. Brako and D. M. Newns, Surf. Sci. **108**, 253 (1981).

[5]K. L. Sebastian, V. C. J. Bhasu, and T. B. Grimley, Surf. Sci. **110**, L571 (1981).

[6]J. N. M. van Wunnik, R. Brako, K. Makosi, and D. M. Newns, Surf. Sci. **126**, 618 (1983).

[7]J. E. Inglesfield, Surf. Sci. **127**, 555 (1983).

[8]D. M. Newns, K. Makoshi, R. Brako, and J. N. M. van Wunnik, Phys. Scr. **T6**, 5 (1983).

[9]L. K. Verhey, B. Poelsema, and A. L. Boers, Nucl. Instrum. Methods **132**, 565 (1976).

[10]R. Souda, M. Aono, C. Oshima, S. Otani, and Y. Ishizawa, Surf. Sci. **150**, L59 (1985); **176**, 657 (1986).

[11]R. Souda and M. Aono, Nucl. Instrum. Methods B **15**, 114 (1986).

[12]T. M. Thomas, H. Neumann, A. W. Czanderna, and J. R. Pitts, Surf. Sci. **175**, L737 (1986).

[13]V. Fano and W. Lichten, Phys. Rev. Lett. **14**, 627 (1965).

[14]M. Barat and W. Lichten, Phys. Rev. A **6**, 211 (1972).

[15]J. P. Gauyacq, J. Phys. B **11**, 85 (1978).

[16]J. P. Gauyacq, J. Phys. B **11**, L217 (1978).

[17]C. Courbin-Gaussorgues and V. Sidis, J. Phys. B **18**, 699 (1985).

[18]C. Kubach and V. Sidis, Phys. Rev. A **14**, 152 (1976).

[19]M. Tsukada, S. Tsuneyuki, and N. Shima, Surf. Sci. **164**, L811 (1985); **169**, 471 (1986).

[20]S. Tsuneyuki and M. Tsukada, Phys. Rev. B **34**, 5758 (1986).

[21]The $3d$ level of sulfur ($\varepsilon_{S\,3d}$) has been estimated by the extrapolation of the SCF $3d$ atomic levels of Sn, Ti, and V atoms given by Herman and Skillmann (Ref. 23). It is found to lie near the vacuum level. The $1s$ level of helium ($\varepsilon_0=\varepsilon_{He\,1s}$) has also been taken from Ref. 23. Thus, we get $\Delta=\varepsilon_{S\,3d}-\varepsilon_0 \simeq 0.87$ a.u. ($\simeq 23.7$ eV) for the He→Si case. We further assumed that $\varepsilon_0=-20$ eV below ε_F, because the energy loss $\delta E \simeq 20$ eV (Ref. 10).

[22]D. M. Newns, Phys. Rev. **178**, 1123 (1969).

[23]F. Herman and S. Skillmann, *Atomic Structure Calculations* (Prentice-Hall, New Jersey, 1963).

[24]R. Souda (private communication).